

## Synthesis and evaluation of isatin derivatives as effective SARS coronavirus 3CL protease inhibitors

Li-Rung Chen,<sup>a</sup> Yu-Chin Wang,<sup>a</sup> Yi Wen Lin,<sup>a</sup> Shan-Yen Chou,<sup>a</sup> Shyh-Fong Chen,<sup>a,\*</sup>  
Lee Tai Liu,<sup>a,\*</sup> Ying-Ta Wu,<sup>b</sup> Chih-Jung Kuo,<sup>b</sup> Tom Shieh-Shung Chen,<sup>a</sup>  
and Shin-Hun Juang<sup>a,\*</sup>

<sup>a</sup>Development Center for Biotechnology, 102, Lane 169, Kang Ning St., Xi Zhi 221, Taipei, Taiwan, ROC

<sup>b</sup>Institute of Biological Chemistry and the Genomic Research Center, Academia Sinica, Nang Gang 11529, Taipei, Taiwan, ROC

Received 10 March 2005; revised 8 April 2005; accepted 14 April 2005

Available online 17 May 2005

**Abstract**—*N*-Substituted isatin derivatives were prepared from the reaction of isatin and various bromides via two steps. Bioactivity assay results (in vitro tests) demonstrated that some of these compounds are potent and selective inhibitors against SARS coronavirus 3CL protease with IC<sub>50</sub> values ranging from 0.95 to 17.50 μM. Additionally, isatin **4o** exhibited more potent inhibition for SARS coronavirus protease than for other proteases including papain, chymotrypsin, and trypsin.  
© 2005 Elsevier Ltd. All rights reserved.

Severe Acute Respiratory Syndrome (SARS) is a new viral atypical pneumonia. This infectious disease originated in Southern China and Hong Kong in late 2002, and then rapidly spread to over 25 countries.<sup>1</sup> The most common symptoms of SARS are cough, high fever (>38 °C), chills, rigor, myalgia, headache, dizziness, as well as progressive radiographic changes of the chest and lymphopenia. The disease had a quite high mortality rate (up to 15–19%) during the initial outbreak. Death may result from progressive respiratory failure owing to alveolar damage. In early 2003, a novel human coronavirus was identified as the causative agent of SARS, and the virus was named SARS coronavirus (SARS CoV).<sup>2</sup> To date, no effective antiviral drug or vaccine has been marketed for treating SARS, although steroid and ribavirin have been used empirically in hospitals of Hong Kong,<sup>3,4</sup> and an HIV protease inhibitor nelfinavir could decrease the replication of SARS CoV in a preliminary in vitro examination.<sup>5</sup>

From the viewpoint of drug design, the human CoV main protease should be an attractive target due to its importance in the cleavage of the CoV polyprotein to

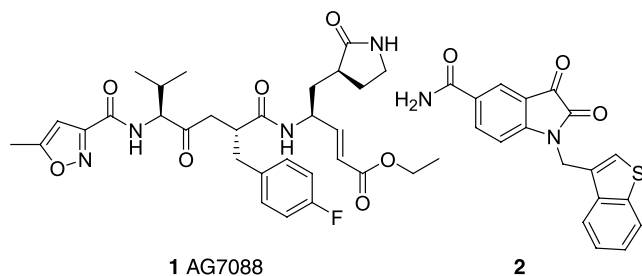
the functional polypeptides.<sup>6</sup> Previous studies have reported that the structure and the active site of human CoV main protease or CoV 3C-like protease (CoV 3CL<sup>PRO</sup>) resemble those of picornavirus 3C protease.<sup>6,7</sup> One of the human rhinovirus (a subtype of picornavirus) 3C protease inhibitor, **1** (AG7088), was previously suggested as a good potential lead compound for the development of SARS CoV 3CL<sup>PRO</sup> inhibitor.<sup>7</sup> However, AG7088 failed to inhibit SARS CoV 3CL<sup>PRO</sup> in vitro at this and other laboratories.<sup>8</sup> Recently, some peptide derivatives have been reported as active inhibitors against SARS CoV 3CL<sup>PRO</sup>.<sup>9a,9b</sup> Several types of small molecules screened from various chemical libraries have been identified as potent SARS coronavirus protease inhibitors with IC<sub>50</sub> values in low micro molar ranges.<sup>9a,9c–9g</sup> However, some of these small molecules may be unsuitable for structural modification because of having complex structures (e.g., sabadinine).<sup>9c</sup> Consequently, innovative scaffolds, which are easy to synthesize and chemically modify must be explored. In this report, preliminary works in the synthesis and evaluation of isatin derivatives as effective SARS CoV 3CL<sup>PRO</sup> inhibitors investigated in our laboratories are described.

It is known that certain isatin (2,3-dioxindole) compounds such as **2** are potent inhibitors against rhinovirus 3C protease.<sup>10</sup> Apparently, the isatin scaffold with derivatization may provide a good candidate for the

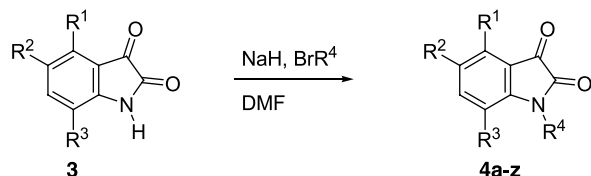
**Keywords:** SARS CoV protease inhibitor; Isatin.

\*Corresponding authors. Tel.: +886 2 26956933; fax: +886 2 26957474; e-mail addresses: [ltliu@mail.dcb.org.tw](mailto:ltliu@mail.dcb.org.tw); [pjuang@mail.dcb.org.tw](mailto:pjuang@mail.dcb.org.tw)

SARS CoV 3CL<sup>pro</sup> inhibitor, because both of the proteases (human SARS CoV and rhinovirus) are cysteine protease and structurally similar at the active site.<sup>7</sup>



The synthesis of *N*-protected isatin derivatives **4** was straightforward. *N*-Alkylation of the corresponding isatin **3**, sodium hydride, and various bromide compounds (transformed from the corresponding alcohol or methyl derivatives) in DMF provided the desired compounds **4a–z** as shown in Scheme 1.<sup>11</sup> Moderate yields (30–



Scheme 1.

60%) were achieved depending on the substituted groups in isatin.

The SARS CoV 3CL<sup>pro</sup> inhibition assays were conducted via fluorescence resonance energy transfer (FRET) according to the reported protocol.<sup>12a</sup> The FRET result was then confirmed through HPLC analysis of the fragment peaks cleaved by 3CL<sup>pro</sup>.<sup>13</sup>

Table 1 lists the in vitro bioactivities of compounds **4a–z** against SARS CoV 3CL protease. The IC<sub>50</sub> values (or percentage of inhibition at 20 μM if the IC<sub>50</sub> value was exceeded 20 μM) in Table 1 were measured via FRET assay.<sup>12a</sup> The bioactivity of these compounds depended on the substituted groups in isatin scaffold and the side chain. The IC<sub>50</sub> values demonstrated that 5-iodo such as **4o** and 7-bromo such as **4k** are the most potent substituted groups in isatin scaffold, and the benzothienophenemethyl side chain provides more inhibitory effect than the benzyl, heterocyclic substituted methyl, and other alkyl groups. Although thiophenecarboxylic 5-chloro-3-pyridinol ester was reported to be a potent inhibitor (IC<sub>50</sub> = 0.5 μM) for SARS protease,<sup>9c</sup> isatins with side chain of thiophenecarboxylic amide **4u** and **4z** exhibited only moderate inhibition effect against SARS-CoV 3CL protease (IC<sub>50</sub> = 12–17 μM).

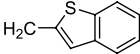
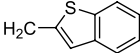
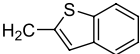
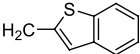
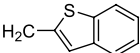
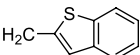
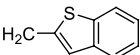
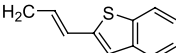
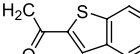
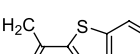
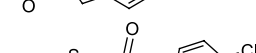
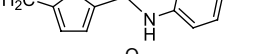
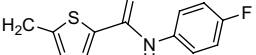
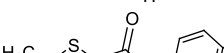
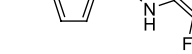
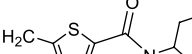
Computer modeling (Fig. 1) showed that compound **4k** and **4o** were fitted into the active pocket of SARS CoV 3CL<sup>pro</sup>.<sup>14</sup> Moreover, the isatin scaffold was docked in

Table 1. Inhibition against SARS CoV 3CL<sup>pro</sup> activity by isatin derivatives **4**

Compound	R <sup>1</sup>	R <sup>2</sup>	R <sup>3</sup>	R <sup>4</sup>	IC <sub>50</sub> or percentage (%) of inhibition at 20 μM <sup>a</sup>
<b>4a</b>	H	C(O)NH <sub>2</sub>	H		25% inhibition at 20 μM
<b>4b</b>	H	CN	H		7.20 μM
<b>4c</b>	H	I	H		9.40 μM
<b>4d</b>	H	I	H		13.50 μM
<b>4e</b>	H	I	H		13% inhibition at 20 μM
<b>4f</b>	H	OCH <sub>3</sub>	H		13% inhibition at 20 μM
<b>4g</b>	H	NO <sub>2</sub>	H		24% inhibition at 20 μM
<b>4h</b>	H	H	H		13.11 μM
<b>4i</b>	H	H	NO <sub>2</sub>		2.00 μM
<b>4j</b>	H	H	NH <sub>2</sub>		31% inhibition at 20 μM

(continued on next page)

Table 1 (continued)

Compound	R <sup>1</sup>	R <sup>2</sup>	R <sup>3</sup>	R <sup>4</sup>	IC <sub>50</sub> or percentage (%) of inhibition at 20 μM <sup>a</sup>
4k	H	H	Br		<b>0.98 μM</b>
4l	H	CH <sub>3</sub>	NO <sub>2</sub>		39% inhibition at 20 μM
4m	H	OCH <sub>3</sub>	H		27% inhibition at 20 μM
4n	H	F	H		4.82 μM
4o	H	I	H		<b>0.95 μM</b>
4p	Cl	H	H		11.20 μM
4q	Cl	H	Cl		46% inhibition at 20 μM
4r	H	I	H		23.50 μM
4s	H	NH <sub>2</sub>	H		40% inhibition at 20 μM
4t	H	CH <sub>3</sub>	NO <sub>2</sub>		40% inhibition at 20 μM
4u	H	I	H		12.57 μM
4v	H	I	H		46% at 20 μM
4w	H	I	H		32% at 20 μM
4x	H	I	H		36% at 20 μM
4y	H	I	H		47% at 20 μM
4z	H	I	H		17.50 μM

<sup>a</sup> The IC<sub>50</sub> values of compounds were measured by a quenched fluorescence resonance energy transfer (FRET) method.<sup>12a</sup> The mixture of SARS CoV 3CL<sup>Pro</sup> (50 nM), various concentrations of the compound (from 0 to 20 μM), and a pH 7.5 buffer containing Tris-HCl (12 mM), NaCl (120 mM), EDTA (0.1 mM), DTT (1 mM), β-ME (7.5 mM) was incubated for 10 min at room temperature. Fluorogenic substrate (Dabcyl-KTSAVLQSGFRKME-Edans, 6 μM) was added. The fluorescence change resulted from the reaction was measured by continuous monitoring with Fusion-Alpha Basic Domestic System (excitation at 330 nm, emission at 515 nm). The initial velocities of the inhibited reactions were plotted against the different inhibitor concentrations to obtain the IC<sub>50</sub>.

the S<sub>1</sub> site, and the side chain (R<sup>4</sup>) was located in the S<sub>2</sub> site of CoV 3CL<sup>Pro</sup>. The carbonyl group of isatin and the NH groups in Cys145, Ser144, and Gly143 of protease were hydrogen bonded. On the other hand, steric effect in isatin scaffold is crucial for ensuring inhibitory potency. Therefore, the inhibitors with a bulkier side chain (4u–z) are less potent than compound 4o because of the limited space between the R<sup>4</sup> of isatin and the

His164 and Met165 of protease. Computational studies also demonstrated that the inhibitory potency depended heavily on hydrophobicity and electron affinity of the substituted groups in isatin. For example, compounds with nonpolar and more electron withdrawing groups such as bromo and nitro in R<sup>3</sup> (4i and 4k) are significantly more potent than the compound with an amino group in R<sup>3</sup> (4j).

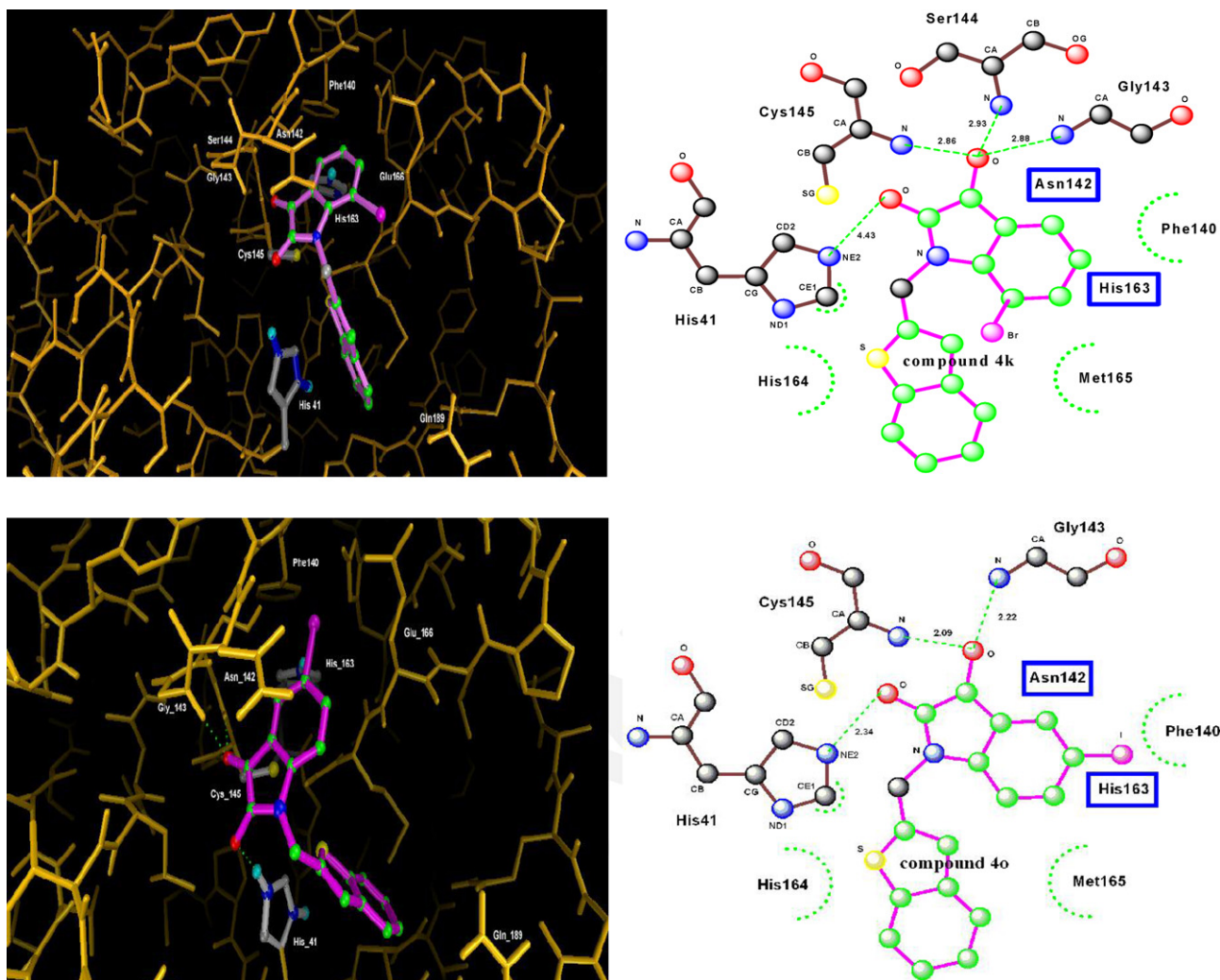


**Figure 1.** Computer modeling of compound **4k** (top) and **4o** (bottom) binding to SARS CoV 3CL<sup>PRO</sup> (Hydrogen bonding between isatin and protease is displayed in the right figure; green: carbons in isatin, blue: nitrogen, red: oxygen.)

Table 2 shows that both isatin **4k** and **4o** exhibited more potent inhibition for SARS CoV 3CL<sup>PRO</sup> than for other proteases such as papain (90–105 times) and trypsin (243–369 times). However, isatin **4k** inhibited chymotrypsin at unexpectedly low IC<sub>50</sub> value compared with compound **4o** (10.4 μM vs 1.00 mM). Consequently, **4k** is less specific for SARS CoV 3CL<sup>PRO</sup> than **4o**. Computer docking of compound **4o** has slightly better (0.2 kcal/mol) binding affinity for SARS CoV 3CL<sup>PRO</sup>. The slight difference might be the reason that compound **4o** is more specific than compound **4k** for other proteases.

In conclusion, a series of *N*-substituted isatin derivatives were simply prepared from isatin, sodium hydride, and various bromide derivatives. The inhibition activities of these compounds against SARS CoV 3CL<sup>PRO</sup> were assessed by FRET and then confirmed via HPLC analysis. The IC<sub>50</sub> values demonstrated that these isatin derivatives inhibited SARS CoV 3CL<sup>PRO</sup> in low micro molar range (0.95–17.50 μM). To our knowledge, compound **4o** is one of the most potent and selective SARS CoV 3CL<sup>PRO</sup> inhibitor reported to date.

**Table 2.** Selective inhibition (IC<sub>50</sub>) against various protease by isatin derivatives **4k** and **4o**<sup>a</sup>

Entry	SARS CoV 3CL <sup>PRO</sup> <sup>b</sup> (cysteine protease)	Papain <sup>c</sup> (cysteine protease)	Chymotrypsin <sup>d</sup> (serine protease)	Trypsin <sup>e</sup> (serine protease)
<b>4k</b>	0.98 μM	103.00 μM	10.40 μM	362.40 μM
<b>4o</b>	0.95 μM	87.24 μM	1.00 mM	243.30 μM

<sup>a</sup> The IC<sub>50</sub> values were measured by FRET as in Table 1.

<sup>b</sup> Substrate (6 μM) and SARS CoV 3CL<sup>PRO</sup> (50 nM).

<sup>c</sup> Substrate (10 μM) and papain (13.3 nM).

<sup>d</sup> Substrate (200 μM) and chymotrypsin (5 nM).

<sup>e</sup> Substrate (200 μM) and trypsin (9 nM).



### Acknowledgments

The financial support from the Ministry of Economy Affairs of ROC and the NMR analytical support provided by Ms. M. H. Lee are greatly appreciated.

### References and notes

- Lee, N.; Hui, D.; Wu, A.; Chan, P.; Cameron, P.; Joynt, G. M.; Ahuja, A.; Yung, M. Y.; Leung, C. B.; To, K. F.; Lui, S. F.; Szeto, C. C.; Chung, S.; Sung, J. J. Y. *N. Engl. J. Med.* **2003**, *348*, 1986.
- Drosten, C.; Günther, S.; Preiser, W.; van der Werf, S.; Brodt, H.-R.; Becker, S.; Rabenau, H.; Panning, M.; Kolesnikova, L.; Fouchier, R. A. M.; Berger, A.; Burguière, A. M.; Cinatl, J.; Eickmann, M.; Escriou, N.; Grywna, K.; Kramme, S.; Manuguerra, J.-C.; Müller, S.; Rickerts, V.; Stürmer, M.; Vieth, S.; Klenk, H.-D.; Osterhaus, A. D. M. E.; Schmitz, H.; Doerr, H. W. *N. Engl. J. Med.* **2003**, *348*, 1967.
- So, L. K.-Y.; Lau, A. C. W.; Yam, L. Y. C.; Cheung, T. M. T.; Poon, E.; Yung, R. W. H.; Yuen, K. Y. *Lancet* **2003**, *361*, 1615.
- Hon, K. L. E.; Leung, C. W.; Cheng, W. T. F.; Chan, P. K. S.; Chu, W. C. W.; Kwan, Y. W.; Li, A. M.; Fong, N. C.; Ng, P. C.; Chiu, M. C.; Li, C. K.; Tam, J. S.; Fok, T. F. *Lancet* **2003**, *361*, 1701.
- Yamamoto, N.; Yang, R.; Yoshinaka, Y.; Amari, S.; Nakano, T.; Cinatl, J.; Rabenau, H.; Doerr, H. W.; Hunsmann, G.; Otaka, A.; Tamamura, H.; Fujii, N.; Yamamoto, N. *Biochem. Biophys. Res. Commun.* **2004**, *318*, 719.
- Anand, K.; Ziebuhr, J.; Wadhwani, P.; Mesters, J. R.; Hilgenfeld, R. *Science* **2003**, *300*, 1763.
- Snijder, E. J.; Bredenbeek, P. J.; Dobbe, J. C.; Thiel, V.; Ziebuhr, J.; Poon, L. L. M.; Guan, Y.; Rozanov, M.; Spaan, W. J. M.; Gorbalenya, A. E. *J. Mol. Biol.* **2003**, *331*, 991.
- Jenwitheesuk, E.; Samudrala, R. *Bioorg. Med. Chem. Lett.* **2003**, *13*, 3989.
- (a) Wu, C.-Y.; Jan, J.-T.; Ma, S.-H.; Kuo, C.-J.; Juan, H.-F.; Cheng, Y.-S. E.; Hsu, H.-H.; Huang, H.-C.; Wu, D.; Brik, A.; Liang, F.-S.; Liu, R.-S.; Fang, J.-M.; Chen, S.-T.; Liang, P.-H.; Wong, C.-H. *PNAS* **2004**, *101*, 10012; (b) Jain, R. P.; Pettersson, H. I.; Zhang, J.; Aull, K. D.; Fortin, P. D.; Huitema, C.; Eltis, L. D.; Parrish, J. C.; James, M. N. G.; Wishart, D. S.; Vederas, J. C. *J. Med. Chem.* **2004**, *47*, 6113; (c) Toney, J. H.; Navas-Martin, S.; Weiss, S. R.; Koeller, A. *J. Med. Chem.* **2004**, *47*, 1079; (d) Bacha, U.; Barrila, J.; Velazquez-Campoy, A.; Leavitt, S. A.; Freire, E. *Biochemistry* **2004**, *43*, 4906; (e) Blanchard, J. E.; Elowe, N. H.; Fortin, P. D.; Huitema, C.; Cechetto, J. D.; Eltis, L. D.; Brown, E. D. *Chem. Biol.* **2004**, *43*, 1445; (f) Kao, R. Y.; Tsui, W. H. W.; Lee, T. S. W.; Tanner, J. A.; Watt, R. M.; Huang, J.-D.; Hu, L.; Chen, G.; Chen, Z.; Zhang, L.; He, T.; Chan, K.-H.; Tse, H.; To, A. P. C.; Ng, L. W. Y.; Wong, B. C. W.; Tsoi, H.-W.; Yang, D.; Ho, D. D.; Yuen, K.-Y. *Chem. Biol.* **2004**, *43*, 1293; (g) Hsu, J. T.-A.; Kuo, C.-J.; Hsieh, H.-P.; Wang, Y.-C.; Huang, K.-K.; Lin, C. P.-C.; Huang, P.-F.; Chen, X.; Liang, P.-H. *FEBS Lett.* **2004**, *574*, 116.
- Webber, S. E.; Tikhe, J.; Worland, S. T.; Fuhrman, S. A.; Hendrickson, T. F.; Matthews, D. A.; Love, R. A.; Patick, A. K.; Meador, J. W.; Ferre, R. A.; Brown, E. L.; DeLisle, D. M.; Ford, C. E.; Binford, S. L. *J. Med. Chem.* **1996**, *39*, 5072.
- All of the new compounds were characterized. The spectra of the active new compounds are reported here. Compound **4k**:  $^1\text{H NMR}$  ( $\text{CDCl}_3$ )  $\delta$  7.67 (m, 1H), 7.61 (m, 2H), 7.54 (d,  $J = 7.3$  Hz, 1H), 7.25–7.18 (m, 3H), 6.94 (d,  $J = 7.5$  Hz, 1H), 5.60 (s, 2H). Compound **4o**:  $^1\text{H NMR}$  ( $\text{CDCl}_3$ )  $\delta$  7.90 (m, 1H), 7.82 (dd,  $J = 8.3, 1.7$  Hz, 1H), 7.75 (d,  $J = 7.7$  Hz, 1H), 7.71 (d,  $J = 7.4$  Hz, 1H), 7.40–7.25 (m, 3H), 6.77 (d,  $J = 8.3$  Hz, 1H), 5.15 (s, 2H). MS (EI)  $m/z$  419  $\text{M}^+$ .
- (a) Kuo, C.-J.; Chi, Y.-H.; Hsu, J. T.-A.; Liang, P.-H. *Biochem. Biophys. Res. Commun.* **2004**, *318*, 862; (b) Blanchard, J. E.; Elowe, N. H.; Huitema, C.; Fortin, P. D.; Cechetto, J. D.; Eltis, L. D.; Brown, E. D. *Chem. Biol.* **2004**, *11*, 1445.
- Substrate (Dabcyl-KTSAVLQSGFRKME-Edans) and the fragments (Dabcyl-KTSAVLQ, Edans-EMKRFSGS) were analyzed by HPLC: Photodiarray detector monitored at UV 300 and 500 nm; reversed phase column COSMOSIL 5C18-MS 4.5 mm  $\times$  150 mm; 0.1% trifluoroacetic acid in acetonitrile/0.1% trifluoroacetic acid in water (10/90, v/v) for 20 min followed by a linear gradient to 0.1% trifluoroacetic acid in acetonitrile/0.1% trifluoroacetic acid in water (45/55, v/v) at the flow rate of 1.0 mL/min. A similar result has been reported during our research: Fan, K.; Wei, P.; Feng, Q.; Chen, S.; Huang, C.; Ma, L.; Lai, B.; Pei, J.; Liu, Y.; Chen, J.; Lai, L. *J. Biol. Chem.* **2004**, *279*, 1637.
- Docking experiments were conducted by using Autodock 3.0.5 with a Lamarckian Genetic Algorithm (LGA).<sup>15</sup> The crystal structure of SARS coronavirus 3CL protease complex with (coded luk4) was obtained from The Protein Databank (PDB: <http://www.rcsb.org/pdb/>). Only chain-A of the dimer was used in this simulation. The structures of isatin derivatives were built in CAChe (Fujitsu, Japan) and refined by performing an optimized geometry calculation in Mechanics using augmented MM2 parameters and stored in PDB format. MGL-TOOLS (MGL, Scripps Institute) was used for structure preparation and parameter creation to meet the input requirements of Autodock. Briefly, essential hydrogen atoms were added to the model structure of 3CL protease (chain A) along with Kollman united atom charges, and solvation parameters. Molecules were added all-hydrogen atoms, assigned Gasteiger–Marsili charges,<sup>16</sup> merge non-polar H atoms, and defined torsions. Autogrid tool in Autodock3.0.5 was applied to compute energy grids (60  $\times$  60  $\times$  70 in  $xyz$  directions with 0.375 Å spacing) of various compound atoms. Grip maps were centered at the active site. Solis and Wets' local search method with LGA was applied to generate available conformations of compound structures within the active site. During docking experiments, each compound was kept flexible (except for the rings and amide bonds) and the protein was rigid.
- Morris, G. M.; Goodsell, D. S.; Halliday, R. S.; Huey, R.; Hart, W. E.; Belew, R. K.; Olson, A. J. *J. Comput. Chem.* **1998**, *19*, 1639.
- Gasteiger, J.; Marsili, M. *Tetrahedron* **1980**, *36*, 3219.